

Magnetic and Structural Properties of Dimeric Bis(acetylacetonato)nickel(II) Isopropanol

CHARLES J. O'CONNOR, EDWIN D. STEVENS

Department of Chemistry, University of New Orleans, New Orleans, La. 70148, U.S.A.

CLARENCE E. PFLUGER

Department of Chemistry, Syracuse University, Syracuse, N.Y. 13210, U.S.A.

and KENT A. KLANDERMAN

Department of Chemistry, State University of New York College at Cortland, Cortland, N.Y. 13045, U.S.A.

Received April 29, 1983

The crystal structure and magnetic properties of bis(acetylacetonato)nickel(II) recrystallized from isopropanol are reported. The complex crystallizes as a dimer containing coordinated iso-propanol ligands with bridging and non bridging acetylacetonato groups. The magnetic susceptibility data exhibit a maximum around $T = 22$ K. The magnetic data were fit to the theoretical equation with the values $g = 2.40$, $J = -7.6$ cm⁻¹, $D = 0.01$ cm⁻¹. The possible effects of the bridging and chelate geometry on the nature of the magnetic coupling is also discussed. Crystal data for Ni₂O₁₀C₂₆H₄₄: Space group = $P2_1/c$, $a = 9.402(2)$ Å, $b = 8.554(1)$ Å, $c = 20.252(5)$ Å, $\beta = 109.79(2)^\circ$, $Z = 2$, $R = 2.9\%$ for 2160 reflections.

Introduction

Metal(II) complexes of acetylacetonato (acac) and related chelates have been some of the most widely studied coordination complexes [1–9]. There are several reports of the isolation of solid adducts of M(II)(acac)₂ with coordinated alcohols [6–9]. The only structure reported to date is that of the Ni(acac)₂(EtOH)₂ [9] in which monomeric Ni(acac)₂ is axially coordinated with ethanol molecules. This structure appears to be representative of the geometry of the lower alcohol members of the series Ni(acac)₂(ROH)₂ where R = CH₃, C₂H₅, and possibly n-C₃H₇. These Ni(acac)₂(ROH)₂ complexes crystallize as blue-green needle like crystals from an emerald green colored solution [10].

This study extends the series of Ni(acac)₂(ROH)₂ complexes to the isopropanol adduct, with surprising results. A dimeric complex is found to crystallize from the isopropanol solution of Ni(acac)₂. Magnetic investigations show a significant antiferromagnetic interaction between the two six coordinate dimeric

centers ($J = -7.6$ cm⁻¹). We report here on the complete x-ray crystal structure, the first containing a coordinated iso-propanol ligand, and the magnetic susceptibility from 5–100 K of the complex [Ni(acac)₂(i-prOH)]₂ where i-prOH = iso-propylalcohol.

Experimental

Synthesis

The title complex, [Ni(acac)₂(i-prOH)]₂, was prepared by dissolving anhydrous Ni(acac)₂ in anhydrous isopropanol. The anhydrous Ni(acac)₂ was prepared using the method outlined by Pfluger *et al.* [10]. The solid anhydrous bis(acetylacetonato)nickel(II) readily dissolved in hot isopropanol giving an emerald green solution which upon slow cooling deposited beautiful well developed emerald green crystals. Rapid cooling provided a microcrystalline solid material which was used for magnetic susceptibility studies. The product complex of the formula [Ni(acac)₂i-prOH]₂ was very unstable with respect to iso-propanol loss and displacement by water when the material was exposed to the atmosphere at room temperature. Exposure to the atmosphere was kept to a minimum during magnetic susceptibility measurements and the crystal used for x-ray data collection was sealed in a glass capillary.

Magnetic Susceptibility

A polycrystalline sample of [Ni(acac)₂i-prOH]₂ weighing about 100 mg was measured between 5 and 100 K on an alternating force magnetometer. The instrument and method of operation is described elsewhere [11, 12].

X-Ray

A previous structure solution of [Ni(acac)₂i-prOH] was reported by Pfluger and Klanderman

[19]. The x-ray study presented here represents a solution based on a recently gathered improved data set. A single crystal with approximate dimensions of $0.4 \times 0.4 \times 0.6$ mm was mounted on a CAD-4 diffractometer and reflections scanned using graphite-monochromated $\text{MoK}\alpha$ radiation. Cell dimensions and estimated standard deviations were determined by centering of 25 reflections with $30^\circ < 2\theta < 50^\circ$. Scans of several classes of reflections revealed systematic absences, $h0l: l = 2n + 1$ and $0k0: k = 2n + 1$, uniquely identified the space group as $\text{P2}_1/c$. Crystal data are summarized in Table I.

A total of 3193 reflections in the range $1^\circ < 2\theta < 52^\circ$ were measured using a continuous $\theta:2\theta$ scan. Three standards measured at 2 hour intervals showed a gradual decline of 1.6% during the course of data collection and were used to correct the intensity measurements. An empirical absorption correction was also applied on the basis of intensity measurements of 3 reflections measured at 10° rotation intervals about the scattering vector. Minimum and maximum transmission factors were estimated to be 99.8% and 95.8%, respectively. Corrected intensities were reduced to relative structure factors F_o , in the usual manner.

The position of the Ni atom was determined by the heavy atom method, and two successive difference electron density maps revealed the position of all other atoms except hydrogens. Atomic scattering factors for all atoms and values of f' and f'' for all atoms except hydrogen were taken from International Tables, Vol. 4. The sum $S = \sum w^2(|F_o| - |F_c|)^2$ was

minimized by full-matrix least-squares refinement, where $w = 1/\sigma(F)$ and the standard deviation of an observation was estimated by the expression,

$$\sigma(F^2) = (\sigma_c^2 + (0.03)^2 F^4)^{1/2},$$

where σ_c is the contribution due to counting statistics. Only the 2160 reflections with $F_o > 3\sigma(F)$ were considered 'observed' and included in the refinement.

Several cycles of refinement with isotropic temperature factors yielded $R = 9.0\%$. All atoms without hydrogens attached were then refined with anisotropic temperature factors, and a difference electron density map was calculated. All hydrogen atoms were located in the difference map and included in the refinement with isotropic temperature factors. All other atoms were refined anisotropically. Four more cycles of full-matrix refinement converged at $R = 2.9\%$ and $R_w = 3.6\%$. On the final cycle, the largest parameter shift was 0.17σ and the standard deviation of an observation of unit weight was 1.35. The highest peak in the final difference Fourier map was $0.37 e/\text{\AA}^3$.

Results and Discussion

The final positional and thermal parameters are given in Table II. Tables III and IV contain the bond lengths and angles. The digits in parentheses in the tables are the estimated standard deviations in the least significant figures quoted and were derived from the inverse matrix in the course of least squares refinement calculations. Fig. 1 shows a view of the $[\text{Ni}(\text{acac})_2\text{i-prOH}]_2$ dimeric unit and Fig. 2 shows a stereoscopic pair view of molecular packing of the unit cell.

The structure consists of nickel(II) complexes dimerized through a bridge formed by one oxygen atom of one of the acetylacetonate ligands. The other acetylacetonate ligand acts as a simple chelate to the nickel ion and the sixth coordination position is occupied by the solvent molecule. The dimer possess inversion symmetry. The geometry is similar to the previously reported structure of dimeric bis(acetylacetonato)aquo cobalt(II) [20].

The resulting coordination geometry about Ni is a distorted octahedron. The largest distortion of the octahedron is a result of formation of an intramolecular hydrogen bond between the hydrogen on O5 of the isopropanol molecule and O3' of the non-bridging acetylacetonate ligand (O5...O3', 2.824(2) Å). The isopropanol ligand is pulled away from the ideal octahedral position toward O3' by approximately 7° , resulting in an O5-Ni...Ni' bond angle of $81.91(6)^\circ$. Surprisingly, the nickel-oxygen bond length of the coordinated *iso*-propanol ligand (2.137 Å) is essentially the same as that found (2.140 Å) for coordinated

TABLE I. Crystal and Data Collection Parameters.

Molecular formula (dimer)	$\text{Ni}_2\text{O}_{10}\text{C}_{26}\text{H}_{44}$
Space Group	$\text{P2}_1/c$
a , Å	9.402(2)
b , Å	8.554(1)
c , Å	20.252(5)
β , deg.	109.79(2)
Z	2
M_r	634.0
ρ_{calc} , g cm^{-3}	1.374
ρ_{obs} , g cm^{-3}	1.36(1)
μ , cm^{-1}	12.8
Temperature, K	300(1)
Diffractometer	CAD4
Radiation	$\text{MoK}\alpha$ ($\lambda = 0.71073$ Å)
Monochromator	graphite
Takeoff angle, deg.	2.7
2θ limits, deg.	$1.0 < 2\theta < 52.0$
2θ scan range, deg.	$1.2 + 0.7 \tan\theta$
Scan speed, deg min^{-1}	variable, 0.6–3.3
Data measured	3193
Data observed ($F_o > 3\sigma_F$)	2160
Parameters	260
R	2.9%
R_w	3.6%

TABLE II. Table of Positional Parameters and their Estimated Standard Deviation.

Atom	x	y	z	B(Å ²)
Ni	0.02408(3)	0.07447(4)	0.07556(1)	2.774(6)
O1	0.1424(2)	-0.0526(2)	0.02640(8)	2.96(3)
O2	0.2031(2)	0.0819(2)	0.16417(9)	3.04(4)
O3	-0.0580(2)	-0.1262(2)	0.10027(8)	3.48(4)
O4	-0.0841(2)	0.2029(2)	0.12510(8)	3.50(4)
O5	0.0807(2)	0.2759(2)	0.02719(8)	3.73(4)
C1	0.3513(3)	-0.1784(5)	0.0084(2)	5.53(8)
C2	0.2820(3)	-0.0936(3)	0.0548(1)	3.23(5)
C3	0.3697(3)	-0.0639(4)	0.1233(1)	4.02(6)
C4	0.3300(3)	0.0219(3)	0.1734(1)	3.40(5)
C5	0.4489(3)	0.0460(4)	0.2444(1)	4.78(7)
C6	-0.1658(3)	-0.2978(4)	0.1613(2)	5.20(7)
C7	-0.1250(3)	-0.1362(4)	0.1454(1)	3.56(5)
C8	-0.1624(3)	-0.0098(4)	0.1793(1)	3.98(6)
C9	-0.1443(3)	0.1489(3)	0.1672(1)	3.43(5)
C10	-0.2067(3)	0.2689(4)	0.2044(2)	5.17(7)
C11	0.1705(4)	0.4727(4)	0.1131(2)	5.57(8)
C12	0.1843(3)	0.4042(3)	0.0479(2)	4.32(7)
C13	0.3420(4)	0.3540(5)	0.0539(2)	6.6(1)
H1	0.436(3)	-0.212(4)	0.035(2)	7.9(9)*
H2	0.287(4)	-0.263(5)	-0.022(2)	10.1(1)*
H3	0.353(3)	-0.109(4)	-0.027(2)	6.9(8)*
H4	0.465(3)	-0.104(3)	0.139(1)	4.5(7)*
H5	0.482(4)	0.150(5)	0.249(2)	11.1(1)*
H6	0.414(4)	-0.040(4)	0.276(2)	8.1(1)*
H7	0.533(3)	0.001(4)	0.246(2)	8.0(9)*
H8	-0.261(4)	-0.328(5)	0.129(2)	11.1(1)*
H9	-0.167(4)	-0.311(5)	0.208(2)	9.1(1)*
H10	-0.098(3)	-0.370(4)	0.159(2)	7.7(9)*
H11	-0.210(3)	-0.028(3)	0.208(1)	4.7(6)*
H12	-0.132(3)	0.354(4)	0.217(1)	6.3(8)*
H13	-0.223(3)	0.222(4)	0.244(2)	7.1(9)*
H14	-0.287(3)	0.292(4)	0.174(2)	8.1(9)*
H15	0.080(2)	0.247(3)	-0.008(1)	2.9(5)*
H16	0.070(3)	0.496(4)	0.106(2)	7.6(9)*
H17	0.239(3)	0.556(4)	0.123(2)	7.5(9)*
H18	0.210(4)	0.392(4)	0.150(2)	8.01*
H19	0.150(3)	0.496(3)	0.011(1)	4.6(6)*
H20	0.327(5)	0.356(6)	0.004(2)	14.2(2)*
H21	0.403(3)	0.449(4)	0.067(2)	7.4(9)*
H22	0.374(4)	0.292(4)	0.090(2)	9.01*

Starred atoms were refined isotropically. Anisotropically refined atoms are given in the form of the isotropic equivalent thermal parameter defined as: $(4/3) [a^2B(1,1) + b^2B(2,2) + c^2B(3,3) + a^*b^* \cos(\gamma)B(1,2) + a^*c^* \cos(\beta)B(1,3) + b^*c^* \cos(\alpha)B(2,3)]$.

etahnol in bis(acetylacetonato)-nickel(II) diethanol [10]. The bridging oxygen O1, is not symmetrically bound to the two nickel atoms. The O1-Ni' bond distance, 2.135(1) Å, is significantly longer than the O1-Ni bond distance, 2.040(1) Å, probably due to a short intramolecular contact between the C1 methyl group on the bridging acetylacetonate and O4' of the non-bridging acetylacetonate. The C2-O1-Ni' and O1-Ni'-O4' angles are also larger than the corresponding values across the molecule [135.2(1)°, and 101.8(1)°, compared with 124.6(1)° and

91.3(1)°, respectively]. The Ni...Ni' distance is 3.203(1) Å.

The bridging acetylacetonate ligand has one terminal and one bridging oxygen atom, and shows a pattern of alternating short and long bond distances around the ring. The non-bridging acetylacetonate, with two terminal oxygen atoms, is somewhat more symmetrical. There are no significant intermolecular contacts.

The magnetic susceptibility and effective magnetic movement for $[\text{Ni}(\text{acac})_2 \cdot \text{PrOH}]_2$ are plotted as a

TABLE IIB. Table of General Temperature Factors (\AA^2). (Supplementary Material)

Name	U(1,1)	U(2,2)	U(3,3)	U(1,2)	U(1,3)	U(2,3)
Ni	0.0311(1)	0.0418(2)	0.0350(1)	0.0019(1)	0.01441(9)	-0.0013(1)
O1	0.0300(6)	0.0458(9)	0.0377(7)	0.0041(7)	0.0129(5)	-0.0004(7)
O2	0.0421(8)	0.066(1)	0.0398(8)	0.0057(9)	0.0116(6)	-0.0035(9)
O3	0.0533(8)	0.0425(9)	0.0438(8)	0.0003(8)	0.0260(6)	-0.002(8)
O4	0.0443(7)	0.047(1)	0.0480(8)	0.0011(8)	0.0240(6)	-0.0050(8)
O5	0.0569(9)	0.047(1)	0.0430(8)	-0.0114(8)	0.0240(6)	-0.0082(8)
C1	0.045(1)	0.104(2)	0.057(2)	0.030(1)	0.013(1)	-0.013(2)
C2	0.033(1)	0.045(1)	0.046(1)	0.005(1)	0.0150(8)	0.004(1)
C3	0.035(1)	0.066(2)	0.046(1)	0.012(1)	0.007(1)	0.003(1)
C4	0.038(1)	0.048(1)	0.0041(1)	0.004(1)	0.0113(9)	0.007(1)
C5	0.044(1)	0.089(2)	0.043(1)	-0.005(2)	0.006(1)	0.000(2)
C6	0.085(2)	0.056(2)	0.70(1)	-0.007(1)	0.043(1)	0.008(1)
C7	0.041(1)	0.053(1)	0.043(1)	-0.000(1)	0.0174(9)	0.006(1)
C8	0.054(1)	0.060(2)	0.049(1)	0.000(1)	0.0336(8)	0.001(1)
C9	0.036(1)	0.056(2)	0.041(1)	0.002(1)	0.0166(8)	-0.005(1)
C10	0.069(1)	0.072(2)	0.070(1)	0.007(1)	0.042(1)	-0.011(1)
C11	0.066(2)	0.066(2)	0.071(2)	-0.005(2)	0.013(1)	-0.027(2)
C12	0.054(1)	0.046(2)	0.066(2)	-0.009(1)	0.022(1)	-0.006(1)
C13	0.052(2)	0.101(3)	0.104(2)	-0.003(2)	0.032(1)	0.009(2)

The form of the anisotropic thermal parameter is: $\exp\{-2\pi^2[h^2a^{*2}U(1,1) + k^2b^{*2}U(2,2) + l^2c^{*2}U(3,3) + 2hka^*b^*U(1,2) + 2hla^*c^*U(1,3) + 2klb^*c^*U(2,3)]\}$ where a^* , b^* and c^* are reciprocal lattice constants.

TABLE III. Bond Distances for $[\text{Ni}(\text{acac})_2\text{i-prOH}]_2$.

Atom 1	Atom 2	Distance
Ni	O1'	2.135(1)
Ni	O1	2.040(1)
Ni	O2	2.003(2)
Ni	O3	2.014(2)
Ni	O4	1.985(1)
Ni	O5	2.137(2)
O1	C2	1.290(3)
O2	C4	1.254(3)
O3	C7	1.277(3)
O4	C9	1.259(3)
O5	C12	1.432(3)
C1	C1	1.500(4)
C2	C3	1.375(3)
C3	C4	1.402(4)
C4	C5	1.506(4)
C6	C7	1.499(4)
C7	C8	1.388(4)
C8	C9	1.401(4)
C9	C10	1.505(4)
C11	C12	1.490(4)
C12	C13	1.508(5)
O5	H15	0.76(2)
C1	H1	0.84(4)
C1	H2	1.00(4)
C1	H3	0.93(3)
C3	H4	0.92(3)
C5	H5	0.94(4)
C5	H6	0.82(4)
C5	H7	0.87(4)
C6	H8	0.95(5)

TABLE III (continued)

Atom 1	Atom 2	Distance
C6	H9	0.95(4)
C6	H10	0.90(4)
C8	H11	0.86(3)
C10	H12	0.98(3)
C10	H13	0.94(3)
C10	H14	0.82(4)
C11	H16	0.93(4)
C11	H17	0.94(4)
C11	H18	0.99(4)
C12	H19	1.05(3)
C13	H20	0.97(5)
C13	H21	0.98(4)
C13	H22	0.87(4)

function of temperature in Fig. 3. There is a maximum in the magnetic susceptibility which occurs at about 22 K. The behavior is consistent with interdimer antiferromagnetic coupling between the two spin $S = 1$ nickel(II) centers. The analysis of the magnetic data is complicated by the presence of a crystal field splitting of the $S = 1$ ground state of nickel(II). The spin Hamiltonian which most accurately represents the system is

$$\hat{H} = -2JS_1 \cdot S_2 - D[S_{1z}^2 + S_{2z}^2] + g\mu_B[H \cdot S_1 + H \cdot S_2] \quad (1)$$

The D term in equation 1 represents the usual zero field splitting of the 3A_2 ground state of nickel(II),

TABLE IV. Bond Angles for [Ni(acac)₂i-prOH]₂.

Atom 1	Atom 2	Atom 3	Angle
O1	Ni	O1'	79.85(6)
O1'	Ni	O2	170.97(6)
O1'	Ni	O3	87.05(6)
O1'	Ni	O4	101.76(6)
O1'	Ni	O5	80.92(6)
O1	Ni	O2	91.30(6)
O1	Ni	O3	89.16(6)
O1	Ni	O4	177.85(6)
O1	Ni	O5	86.81(7)
O2	Ni	O3	94.65(7)
O2	Ni	O4	87.04(7)
O2	Ni	O5	96.94(7)
O3	Ni	O4	92.34(6)
O3	Ni	O5	167.81(7)
O4	Ni	O5	92.03(7)
Ni	O1	Ni'	100.15(6)
Ni'	O1	C2	135.2(1)
Ni	O1	C2	124.6(1)
Ni	O2	C4	126.1(2)
Ni	O3	C7	124.0(2)
Ni	O4	C9	124.3(2)
Ni	O5	C12	137.2(2)
O1	C2	C1	116.4(2)
O1	C2	C3	124.9(2)
C1	C2	C3	118.8(2)
C2	C3	C4	127.7(2)
O2	C4	C3	125.4(2)
O2	C4	C5	116.6(3)
C3	C4	C5	118.0(2)
O3	C7	C6	116.1(3)
O3	C7	C8	124.9(2)
C6	C7	C8	119.0(2)
C7	C8	C9	126.9(2)
O4	C9	C8	125.8(2)
O4	C9	C10	115.4(3)
C8	C9	C10	118.8(2)
O5	C12	C11	107.8(3)
O5	C12	C13	111.0(3)
C11	C12	C13	114.7(3)
Ni	O5	H15	105(2)
C12	O5	H15	108(2)
C2	C1	H1	106(3)
C2	C1	H2	116(2)
C2	C1	H3	107(2)
C2	C3	H4	117(2)
C4	C3	H4	115(2)
C4	C5	H5	110(3)
C4	C5	H6	112(3)
C4	C4	H7	111(2)
C7	C6	H8	111(3)
C7	C6	H9	114(3)
C7	C6	H10	113(2)
C7	C8	H11	118(2)
C9	C8	H11	114(2)
C9	C10	H12	106(2)
C9	C10	H13	109(2)
C9	C10	H14	102(3)

TABLE IV. (continued)

Atom 1	Atom 2	Atom 3	Angle
C12	C11	H16	110(2)
C12	C11	H17	104(2)
C12	C11	H18	106(2)
O5	C12	H19	110(2)
C11	C12	H19	104(2)
C13	C12	H19	109(2)
C12	C13	H20	97(3)
C12	C13	H21	105(2)
C12	C13	H22	107(3)
H1	C1	H2	113.(3)
H1	C1	H3	116.(3)
H2	C1	H3	99.(3)
H5	C5	H6	101.(4)
H5	C5	H7	99.(3)
H6	C5	H7	123.(4)
H8	C6	H9	110.(3)
H8	C6	H10	107.(4)
H9	C6	H10	102.(3)
H12	C10	H13	113.(3)
H12	C10	H14	115.(3)
H13	C10	H14	111.(3)
H16	C11	H17	117.(3)
H16	C11	H18	112.(3)
H17	C11	H18	108.(3)
H20	C13	H21	97.(4)
H20	C13	H22	141.(5)
H21	C13	H22	106.(4)

following the sign convention that a positive D corresponds to the doublet ($M_s = 1$) below the singlet ($M_s = 0$). The equations for the magnetic susceptibility have been derived from the Hamiltonian in equation (1) using the Van Vleck equation by Ginsberg *et al.* [13]. The equation reported by these authors includes a provision for inter-dimer magnetic exchange but this term was not needed in our analysis. The equation reported is lengthy and will not be reproduced here. It may be represented by $\chi(g, J, D)$ and this equation was used in the analysis of the magnetic data of [Ni(acac)₂i-prOH]₂. The curve through the data points in Fig. 3 represents the best fit of the data to $\chi(g, J, D)$ with the following parameters, $g = 2.4$, $J = -7.6 \text{ cm}^{-1}$, $D = 0.01 \text{ cm}^{-1}$.

The magnitude of the antiferromagnetic coupling is reasonably large and it is interesting to draw some structural comparisons with similar nickel(II) dimers. A recent study by Butcher *et al.* [14] has shown that the orientation of a bridging chelate has a marked effect on the sign of the coupling. Two types of bridging chelate orientations are shown in Fig. 4, each having inversion symmetry. In 1, [14–17] the plane of the bridging chelate is oriented perpendicular to the plane of the Ni₂O₂ bridge and the complex

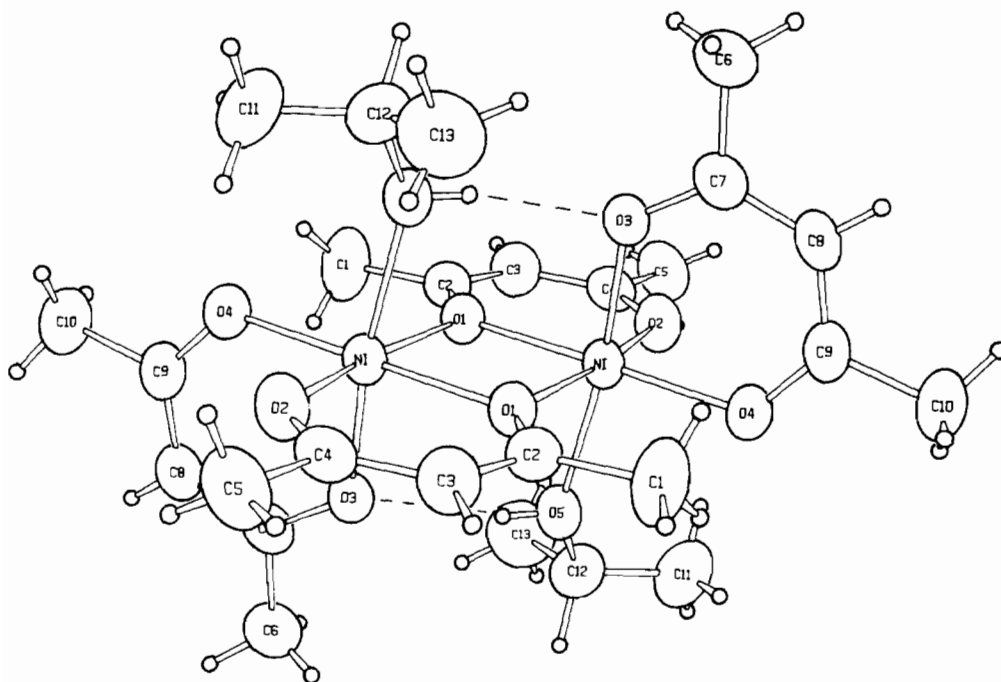


Fig. 1. ORTEP drawing of the dimeric molecular unit of $[\text{Ni}(\text{acac})_2\text{i-prOH}]_2$.

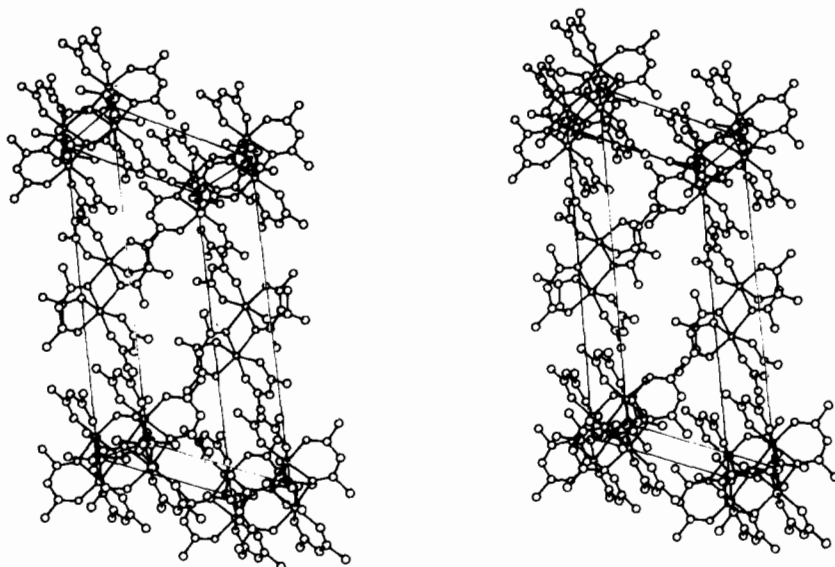


Fig. 2. Stereoscopic pair packing diagram of $[\text{Ni}(\text{acac})_2\text{i-prOH}]_2$.

exhibits ferromagnetic coupling. In the case of 2 [14–18] the bridging plane is oriented parallel and coplanar with the Ni_2O_2 bridging plane and the complex is antiferromagnetically coupled. The complex reported here, $[\text{Ni}(\text{acac})_2\text{i-prOH}]_2$, fits into category 2 structurally and magnetically.

The changes in sign of magnetic coupling caused by the structural change from type 1 to type 2 bridging may be explained in terms of the electronic

orbitals on the oxygen. In type 1 complexes, the p_z orbital on the bridging oxygen may interact with each of the two metals only via a π -overlap. In the type 2 complexes, the p_z orbital on the bridging oxygen may interact with the two nickel(II) centers via a σ -overlap to one nickel(II) ion and a π -overlap to the other. The former case results in antiferromagnetic exchange. There are an insufficient number of complexes from which to draw

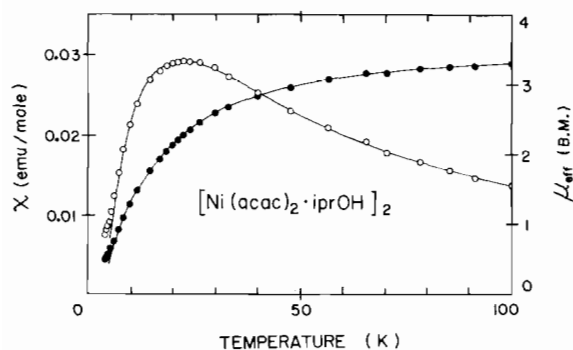
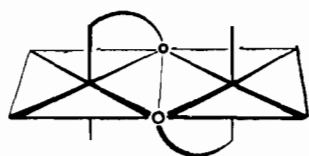
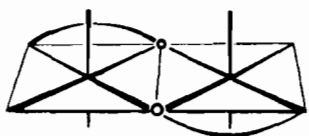


Fig. 3. Magnetic susceptibility and effective magnetic moment of $[\text{Ni}(\text{acac})_2 \cdot \text{iPrOH}]_2$ plotted as a function of temperature. The smooth line through the data points is the best fit of the equation to the Ginsberg model as described in the text.



1



2

Fig. 4. Schematic drawing of binuclear coordination spheres showing the bridging ligand perpendicular to the bridging plane (1) and the bridging ligand coplanar to the bridging plane (2).

structural correlations within the type 1 or type 2 subsets; however, as the number of examples increases some useful correlations may evolve.

References

- 1 C. J. O'Connor and R. L. Carlin, *Inorg. Chem.*, **14**, 291 (1975).
- 2 A. P. Ginsberg, R. L. Martin and R. C. Sherwood, *Inorg. Chem.*, **1**, 932 (1968).
- 3 G. J. Bullen, R. Mason and P. Pauling, *Inorg. Chem.*, **4**, 456 (1965).
- 4 M. D. Glick and K. L. Lintvedt, *Prog. Inorg. Chem.*, **21**, 233 (1977).
- 5 R. H. Holm and M. J. O'Connor, *Prog. Inorg. Chem.*, **14**, 241 (1971).
- 6 D. P. Graddon and G. M. Mockler, *Aust. J. Chem.*, **17**, 1119 (1964).
- 7 D. P. Graddon and E. C. Watton, *Nature (London)*, **190**, 906 (1961).
- 8 P. E. Rakita, S. J. Kopperl and J. P. Fackler, *J. Inorg. Nucl. Chem.*, **30**, 2139 (1968).
- 9 W. R. Walker and N. C. Li, *J. Inorg. Nucl. Chem.*, **27**, 2255 (1965).
- 10 C. E. Pfluger, T. S. Burke and A. L. Bednowitz, *J. Cryst. Mol. Struct.*, **3**, 181 (1973).
- 11 C. J. O'Connor, *Prog. Inorg. Chem.*, **29**, 203 (1982).
- 12 C. J. O'Connor, C. L. Klein, L. M. Trefonas and R. J. Majeste, *Inorg. Chem.*, **20**, 3486 (1981).
- 13 A. P. Ginsberg, R. L. Marten, R. W. Brookes and R. C. Sherwood, *Inorg. Chem.*, **11**, 2884 (1972).
- 14 R. J. Butcher, C. J. O'Connor and E. Sinn, *Inorg. Chem.*, **20**, 3486 (1981).
- 15 R. J. Butcher and E. Sinn, *J. Chem. Soc. Chem. Commun.*, 832 (1975).
- 16 R. J. Butcher, J. Jasinski, G. M. Mockler and E. Sinn, *J. Chem. Soc., Dalton Trans.*, 1099 (1976).
- 17 R. J. Butcher and E. Sinn, *Aust. J. Chem.*, **32**, 331 (1979).
- 18 C. J. O'Connor and E. Sinn, to be submitted for publication.
- 19 C. E. Pfluger and K. A. Klanderman, *Amer. Cryst. Assoc. Spring Meeting*, Abst. papers, 11 (1975).
- 20 F. A. Cotton and R. C. Elder, *Inorg. Chem.*, **5**, 423 (1966).